ELSEVIER

Journal of Organometallic Chemistry 655 (2002) 39–48

Journal of Organometallic Chemistry

www.elsevier.com/locate/jorganchem

Synthesis, characterization and theoretical studies of new heterometallic carbonyl clusters bridged by 4,4′-dipyridyl unit

Wai-Yeung Wong [a,*], Suk-Ha Cheung [a], Xin Huang [b], Zhenyang Lin [b]

[a] *Department of Chemistry, Hong Kong Baptist University, Waterloo Road, Kowloon Tong, Hong Kong, PR China*
[b] *Department of Chemistry, The Hong Kong University of Science and Technology, Clearwater Bay, Hong Kong, PR China*

Received 28 January 2002; received in revised form 15 March 2002; accepted 15 March 2002

Abstract

4,4′-Bipyridine (4,4′-bipy) reacts with the activated cluster $[Os_3(CO)_{10}(NCMe)_2]$ readily at room temperature to give a mixture of $[Os_3(\mu\text{-}H)(CO)_{10}(\mu\text{-}NC_5H_3C_5H_4N)]$ (**1**) and $[Os_3(\mu\text{-}H)(CO)_{10}(\mu\text{-}NC_5H_3C_5H_3N)Os_3(\mu\text{-}H)(CO)_{10}]$ (**2**), the composition of which depends upon the reaction conditions and the ratio of the reactants. The reactivities of the metalloligand precursor **1** with a pendant nitrogen atom towards $[W(CO)_5(THF)]$ and $[Re(CO)_5Cl]$ have been investigated, affording two new heterometallic clusters $[Os_3(\mu\text{-}H)(CO)_{10}(\mu\text{-}NC_5H_3C_5H_4N)W(CO)_5]$ (**3**) and $[ReCl(CO)_3\{Os_3(\mu\text{-}H)(CO)_{10}(\mu\text{-}NC_5H_3C_5H_4N)\}_2]$ (**4**) in moderate to good yields. Compound **4** can also be prepared from the reaction between $[Os_3(CO)_{10}(NCMe)_2]$ and $[ReCl(CO)_3(4,4'\text{-bipy})_2]$. The X-ray crystal structures of compounds **1**–**3** have been determined and molecular orbital calculations on these complexes using density functional theory (DFT) method reveal that they all have similar orbitals in the LUMO region. Clusters **1** and **2** have the Os–Os σ-bonding orbitals as their HOMO orbitals while cluster **3** has the 't_{2g}' set orbitals of the $W(CO)_5$ fragment as the HOMO orbitals.

Keywords: Clusters; Crystal structures; Tungsten; Rhenium; Molecular orbital calculations

1. Introduction

Metal complexes containing bridging 4,4′-bipyridine (4,4′-bipy) ligand or alike continue to arouse constant and general interest in coordination and metallosupramolecular chemistry [1]. Linking transition metal centres together with these ligands allows communication between them, usually leading to intriguing physical properties [1,2]. Among these, 4,4′-bipyridine and pyrazine have found extensive use in this context in the assembly of rectangular two-dimensional metal network structures and coordination polymers with interesting structural motifs [3]. A variety of solid-state architectures have been constructed in the past years based on these excellent bridging units [3,4]. We have also recently reported the use of 4,4′-azopyridine in the preparation of some homometallic linking osmium cluster complexes and dinuclear tungsten carbonyl species [5]. Taking into account the fact that the symmetrical rigid 4,4′-bipy ligand could serve as a versatile building block for the construction of metal–organic coordination frameworks and has the potential of linking up two different metal moieties within a single molecule, we initiated a program to develop a promising synthetic path in the search for a new class of stable heterometallic carbonyl compounds bridged by dipyridyl ligands. Here, we present the results of such a study. In the first place, the new metalloligand complex $[Os_3(\mu\text{-}H)(CO)_{10}(\mu\text{-}NC_5H_3C_5H_4N)]$ (**1**) possessing one functional coordination site was synthesized and its subsequent use in the generation of new homonuclear and heteronuclear linked species will be discussed. Such compounds are thought to be good intermediates in the synthesis and build-up of high-nuclearity clusters and supramolecular coordination compounds [6].

* Corresponding author. Fax: +852-3411-7348.
E-mail address: rwywong@hkbu.edu.hk (W.-Y. Wong).

0022-328X/02/$ - see front matter
PII: S0022-328X(02)01410-9

2. Results and discussion

2.1. Synthesis

Depending on the reaction conditions and stoichiometry of the reactants used, the complex $[Os_3(\mu\text{-}H)(CO)_{10}(\mu\text{-}NC_5H_3C_5H_4N)]$ (**1**) with a pendant pyridyl group at the periphery and the linking cluster $[Os_3(\mu\text{-}H)(CO)_{10}(\mu\text{-}NC_5H_3C_5H_3N)Os_3(\mu\text{-}H)(CO)_{10}]$ (**2**) can be prepared with varying yields by the reaction of $[Os_3(CO)_{10}(NCMe)_2]$ with 4,4′-bipy (Scheme 1). Complexes **1** and **2** are actually oxidative-addition products from this reaction. They are the results of orthometallation of the pyridyl ring in the ligands accompanied by C–H bond cleavage α to the nitrogen donor site and loss of MeCN groups [6b,6c,7]. The use of complex **1** as a metalloligand can lead to the synthesis of several homometallic and heterometallic carbonyl clusters. Cluster **2** can be alternatively made by reacting complex **1** with another molar equivalent of $[Os_3(CO)_{10}(NCMe)_2]$. The facile displacement of one carbonyl ligand of $[W(CO)_6]$ by pyridines to give $[W(CO)_5(NC_5H_4R)]$ is well-documented and has successfully been applied to the preparation of $[Os_3(\mu\text{-}H)(CO)_{10}(\mu\text{-}NC_5H_3C_5H_4N)W(CO)_5]$ (**3**) [5,8]. The monosubstituted tungsten carbonyl complex **3** was readily prepared by reacting **1** with $[W(CO)_5(THF)]$ prepared in situ from photolysis of $[W(CO)_6]$ in THF. Moreover, substitution of two CO ligands in $[ReCl(CO)_5]$ by pyridyl ligands is highly feasible [9] and this provides a convenient synthetic entry to the preparation of $[ReCl(CO)_3\{Os_3(\mu\text{-}H)(CO)_{10}(\mu\text{-}NC_5H_3C_5H_4N)\}_2]$ (**4**). Complex **4** can also be prepared with a similar yield by treatment of $[Os_3(CO)_{10}(NCMe)_2]$ with the rhenium bis(dipyridyl) species $[ReCl(CO)_3(4,4'\text{-bipy})_2]$. The reactions were readily monitored by thin-layer chromatography (TLC) and solution IR spectroscopy. All the complexes obtained were purified by preparative TLC on silica using a hexane–CH_2Cl_2 mixture as eluent and they were isolated as air-stable yellow to orange solids in high purity. Complexes **1**–**4** are soluble in common organic solvents and have been characterized by satisfactory microanalysis, fast atom bombardment mass spectrometry (FABMS), IR and NMR spectroscopies. The molecular structures of **1**–**3** have been established by X-ray crystallography.

2.2. Spectroscopic properties

The molecular formulae of all the new complexes was initially established by FABMS, IR and ^{1}H-NMR spectroscopies. The spectroscopic properties are in accordance with their formulation and the data are summarized in Table 1. In the solution IR spectra, the ν_{CO} vibrational modes are diagnostic and represent a useful monitoring tool. For **1** and **2**, their IR carbonyl spectra in CH_2Cl_2 solution have a similar ν_{CO} pattern in the region 2200–1600 cm^{-1} and are reminiscent of the μ-pyridyl clusters $[Os_3(\mu\text{-}H)(CO)_{10}(\mu\text{-}NC_5H_3R)]$ (R = H, alkyl, anthryl, ferrocenyl derivatives, etc.) [6c,7,10] and of other related orthometallated nitrogen-hetero-

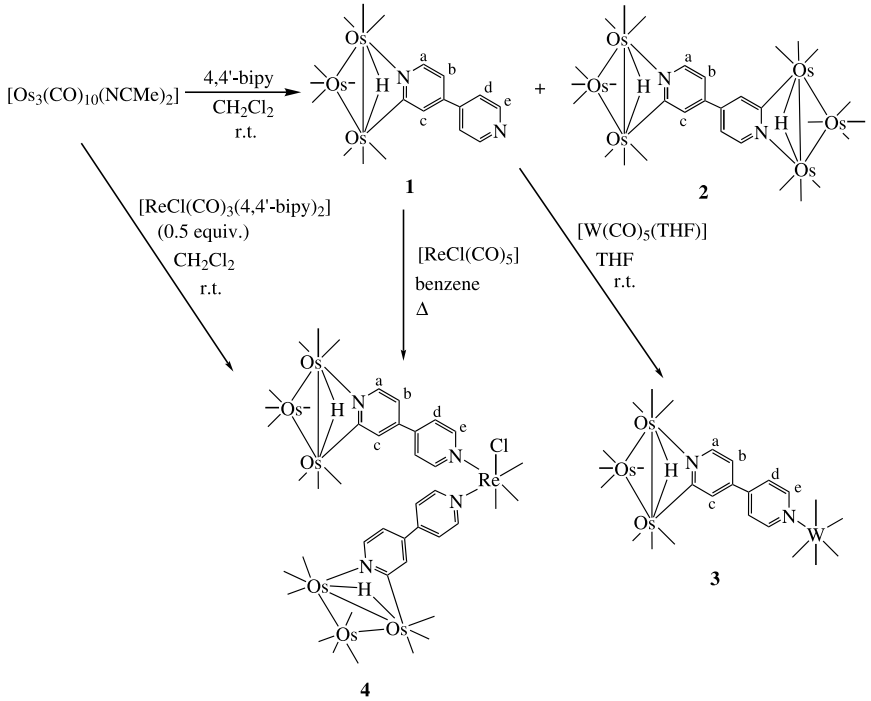

Scheme 1.

Table 1
Spectroscopic data for compounds **1**–**4**

Complex	IR (ν_{CO})/cm^{-1} [a]	^{1}H-NMR (δ, J in Hz) [b]	MS (m/z) [c]
1	2103m, 2064vs, 2052vs, 2018vs, 2010s, 1990m, 1968sh	8.70 (dd, 2H, J = 4.4, 1.6, H_d or H_e) 8.20 (d, 1H, J = 6.1, H_a) 7.50 (d, 1H, J = 1.8, H_c) 7.44 (dd, 2H, J = 4.4, 1.6, H_d or H_e) 6.87 (dd, 1H, J = 6.1, 1.8, H_b) −14.78 (s, 1H, OsH)	1007 (1007)
2	2102m, 2064vs, 2053s, 2019s, 2008s, 1992sh, 1968sh	8.18 (d, 2H, J = 6.1, H_a) 7.38 (m, 2H, H_c) 6.83 (m, 2H, H_b) −14.78 (s, 2H, OsH)	1858 (1858)
3	2104m, 2064vs, 2053vs, 2020s, 2009s, 1991m, 1974sh, 1929vs, 1898m	8.92 (d, 2H, J = 6.7, H_d or H_e) 8.27 (d, 1H, J = 6.1, H_a) 7.47 (d, 1H, J = 2.4, H_c) 7.43 (d, 2H, J = 6.7, H_d or H_e) 6.86 (dd, 1H, J = 6.1, 2.4, H_b) −14.73 (s, 1H, OsH)	1331 (1331)
4	2104m, 2064vs, 2052vs, 2020vs, 2008s, 1992m, 1970w, 1926m, 1890m	8.87 (dd, 4H, J = 5.0, 1.6, H_d or H_e) 8.25 (d, 2H, J = 6.0, H_a) 7.50 (dd, 4H, H_d or H_e) 7.45 (m, 2H, H_c) 6.85 (m, 2H, H_b) −14.76 (s, 2H, OsH)	2319 (2319)

[a] CH_2Cl_2.
[b] $CDCl_3$.
[c] Simulated masses in parentheses.

cyclic compounds [11]. This suggests the N,C mode of binding to the metal atoms. The solution state IR spectrum of **3** in the carbonyl absorption region appears as a simple combination of those found in the constituent species, $[Os_3(\mu\text{-}H)(CO)_{10}(\mu\text{-}NC_5H_3R)]$ and $[W(CO)_5(NC_5H_4R)]$ [5,8a,12].

The ^{1}H-NMR spectra of **1**–**4** show resonances due to the protons associated with the ligands and the bridging hydrides along the metal–metal edges [13]. Their ^{1}H-NMR spectra further confirm orthometallation of the pyridine ring over the Os_3 unit. The most downfield signal is ascribed to the *ortho*-proton which integrates as one proton against the hydride resonance. In each case, the parent molecular ions were detected in their respective positive FAB mass spectra followed by sequential loss of carbonyls.

2.3. Electronic absorption spectroscopy and redox properties

Table 2 lists the electronic spectral data for the new complexes in CH_2Cl_2 at room temperature. The absorption spectra of these compounds are essentially dominated by the intense bands in the UV region that arise from the metal-perturbed intraligand $\pi \rightarrow \pi^*$ transitions. An additional absorption band is also observed near 400 nm for **1**–**3** whereas a broad shoulder at ca. 372 nm is present for **4** which tails off beyond 400 nm. These

Table 2
Electronic absorption and electrochemical data for complexes **1**–**4** in CH_2Cl_2

Compound	λ_{max} (ε) [a]	E (ox)/V [b]
1	230 (4.1), 252 (3.5), 393 (0.9)	0.79 [c]
2	231 (5.6), 274sh (4.4), 396 (1.5)	0.91 [c]
3	243 (7.4), 398 (1.4)	0.83 [c]
4	229 (10.0), 324 (3.3), 372 (2.5) [d]	0.84 [c]

[a] Extinction coefficients ($\times 10^{-4}$) are shown in parentheses.
[b] The electrochemical measurements were made at a glassy carbon working electrode containing 0.1 M $[NBu_4]PF_6$ as base electrolyte, using a scan rate of 100 mV s^{-1}. All potentials were quoted with reference to the ferrocene/ferrocenium couple which was used as an internal standard.
[c] Irreversible wave.
[d] Shoulder band.

lowest energy peaks can be compared with that observed in $[Os_3(\mu\text{-}H)(CO)_{10}(\mu\text{-}NC_5H_4)]$ (386 nm) [6c]. With reference to the results obtained from molecular orbital calculations (vide infra), it is likely that the low-energy features are predominantly of cluster core-to-ligand charge transfer character, in common with those normally present in pyridyl metal complexes [14]. However, we cannot rule out that such low-energy band may be obscured by the $n \rightarrow \pi^*$ transition associated with the pyridyl ligand in **1**. By comparing with the absorption spectrum of *fac*-$[ReCl(CO)_3(4,4'\text{-bipy})_2]$ in CH_2Cl_2

which exhibits the Re→4,4′-bipy charge transfer band at 317 nm [9b], we assign the absorption peak at 324 nm for **4** to arise from a similar MLCT state.

The electrochemical properties of **1**–**4** were studied in CH_2Cl_2 using cyclic voltammetry with $[NBu_4]PF_6$ as the supporting electrolyte and redox potential values obtained are gathered in Table 2. Each of them undergoes an irreversible oxidation in the range 0.79–0.91 V, rather close to the oxidation potential for the pyridyl analogue $[Os_3(\mu\text{-H})(CO)_{10}(\mu\text{-}NC_5H_4)]$ (0.92 V) [6c]. Similar irreversible oxidation processes were also encountered for a series of electron deficient benzoheterocycle triosmium clusters reported by Rosenberg and coworkers [15]. We can thus assign this oxidation event to be cluster-based and attachment of another electron-deficient metal carbonyl fragment to the original cluster **1** incurs an anodic shift in the oxidation potentials for **2** and **3** as compared to that of **1**. No ligand-centred reduction processes were apparent within the solvent window in each case. In contrast to other tungsten carbonyl complexes bearing pyridyl ligands, there is no evidence of observing any oxidation process due to the $\{W(CO)_5(NC_5H_4R)\}$ unit in **3** [5,8a,8b].

2.4. Crystal structure analyses

To substantiate the proposed structures of the newly synthesized compounds, single-crystal X-ray analyses were carried out for **1**–**3**. Perspective views of the molecular structures of **1**–**3** are depicted in Figs. 1–3, respectively, which include the atom-numbering scheme. Pertinent interatomic distances and angles are combined and listed in Table 3. The structure of **1** reveals an orthometallation of one of the pyridyl rings, arising from C–H fission and transfer of an *o*-hydrogen atom to the metal. This is consistent with the structural assignment from spectroscopic studies and is directly related to the structure of the previously reported $[Os_3(\mu\text{-H})(CO)_{10}(\mu\text{-}NC_5H_4R)]$ [6c,7a,10] and other thiolato bridged triosmium clusters of the type $[Os_3(\mu\text{-H})(CO)_{10}(\mu\text{-SR})]$ (R = Et or Ph) formed by oxidative addition reaction of thiols with $[Os_3(CO)_{10}(NCMe)_2]$ [16]. The pyridyl ring bridges the edge Os(2)–Os(3) of the Os_3 triangle to afford a four-membered ring containing Os(2), Os(3), C(11) and N(1) while the other pyridyl binding site remains uncoordinated. For **2**, the ligand links up two Os_3 units in a symmetrical fashion and both ends of 4,4′-bipy have undergone orthometallation. The essential structural feature of the cluster metal core in **2** is similar to that of **1**. The length of the Os(2)–Os(3) edge that is bridged by the hydride and pyridyl plane is longer (2.917(2) **1**, 2.9184(9) Å **2**) than the two non-bridged Os–Os bonds (2.8643(7)–2.8848(7) Å), typical of other similar complexes [6c,7a,10]. The pyridyl rings are essentially planar in each case.

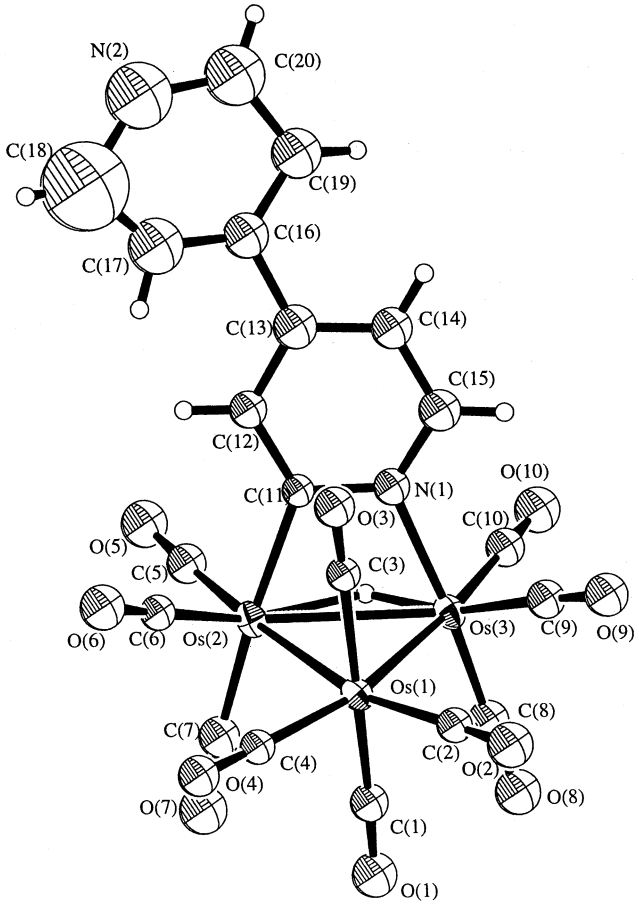

Fig. 1. Molecular structure of **1**, showing the atomic labelling scheme.

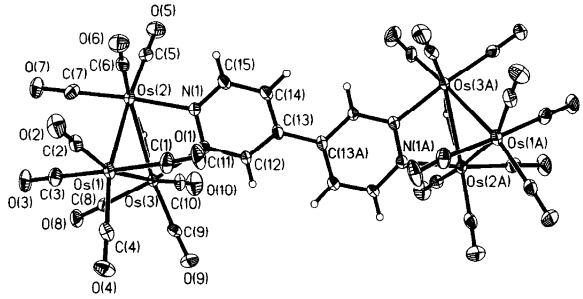

Fig. 2. Molecular structure of **2**, showing the atomic labelling scheme.

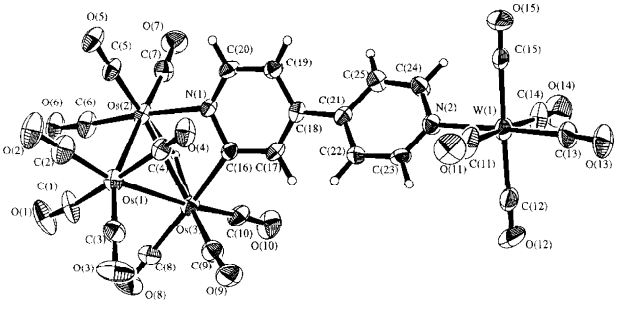

Fig. 3. Molecular structure of **3**, showing the atomic labelling scheme.

Table 3
Selected bond lengths (Å) and angles (°) for complexes **1**–**3**

	1	**2**	**3**
Bond lengths			
Os(1)–Os(2)	2.879(2)	2.8643(7)	2.866(1)
Os(1)–Os(3)	2.874(2)	2.8848(7)	2.8881(9)
Os(2)–Os(3)	2.917(2)	2.9184(9)	2.9271(9)
Os–C(pyridyl)	2.06(3)	2.111(8)	2.09(2)
Os–N(pyridyl)	2.07(2)	2.125(7)	2.14(1)
W(1)–N(2)			2.28(1)
Bond angles			
Os(2)–Os(1)–Os(3)	60.95(4)	61.01(2)	61.15(2)
Os(1)–Os(2)–Os(3)	59.44(4)	59.84(2)	59.79(2)
Os(1)–Os(3)–Os(2)	59.61(4)	59.15(2)	59.05(2)
Os(X)–Os(Y)–N(pyridyl)	68.0(6) ($X=2,\ Y=3$)	68.3(2) ($X=3,\ Y=2$)	69.1(3) ($X=3,\ Y=2$)
Os(X)–Os(Y)–C(pyridyl)	68.3(7) ($X=3,\ Y=2$)	67.8(3) ($X=2,\ Y=3$)	67.7(4) ($X=2,\ Y=3$)
Os(X)–C(Y)–N(pyridyl)	112(1) ($X=2,\ Y=11$)	113.0(6) ($X=3,\ Y=11$)	114(1) ($X=3,\ Y=16$)

Structurally, the heterometallic complex **3** can be treated as comprising compound **1** that is covalently bonded to a $W(CO)_5$ fragment through the dangling pyridine. Within the triosmium cluster framework, the dibridged metal–metal bond is the longest of the three (Os(2)–Os(3) 2.9271(9) Å). The other two non-bridged metal–metal bonds are at 2.866(1) and 2.8881(9) Å. The tungsten atom resides in an approximately octahedral environment and the W–C–O bonds do not show significant deviations from linearity (174(2)–178(1)°). The W–N(pyridyl) distance is 2.28(1) Å, which compares well with literature values [5,8b]. The W–C bond distances range from 2.01(2) to 2.07(2) Å. All the aromatic bond lengths and angles are within the expected range.

2.5. Molecular orbital calculations

To understand the spectroscopic behaviour of these clusters, we have carried out molecular orbital calculations for **1**–**3** at the B3LYP level of density functional theory (DFT) [17] based on their experimental geometries. Examining the molecular orbital patterns of our molecules, we found that the three highest occupied molecular orbitals (HOMOs) correspond to the two unbridged Os–Os σ-bonds and the lone pair on the uncoordinated nitrogen of the 4,4′-dipyridyl ligand for **1**. Likewise, the four HOMOs for **2** correspond to the four unbridged Os–Os σ-bonds, two from each Os_3 cluster unit. For **3**, the five HOMOs belong to the three 't_{2g}' set d orbitals of the $W(CO)_5$ unit and the two unbridged Os–Os σ-bonds. The lowest unoccupied molecular orbitals (LUMOs) delocalize extensively on the dipyridyl ligands for all the three clusters. Fig. 4 shows the contour plots [18] of these frontier molecular orbitals for **1** and **3**. The orbital interaction diagram, shown in Fig. 5 for **1**, illustrates how the $[HOs_3(CO)_{10}]^+$ fragment interacts with the dipyridyl unit. The left column gives the frontier fragment orbitals of $[HOs_3(CO)_{10}]^+$. These frontier orbitals include two occupied Os–Os σ-bonding orbitals and two unoccupied fragment orbitals which are responsible for interactions with symmetry-adapted donor orbitals from the dipyridyl ligand. The right column shows the π and π* orbital energy levels of the dipyridyl ligand together

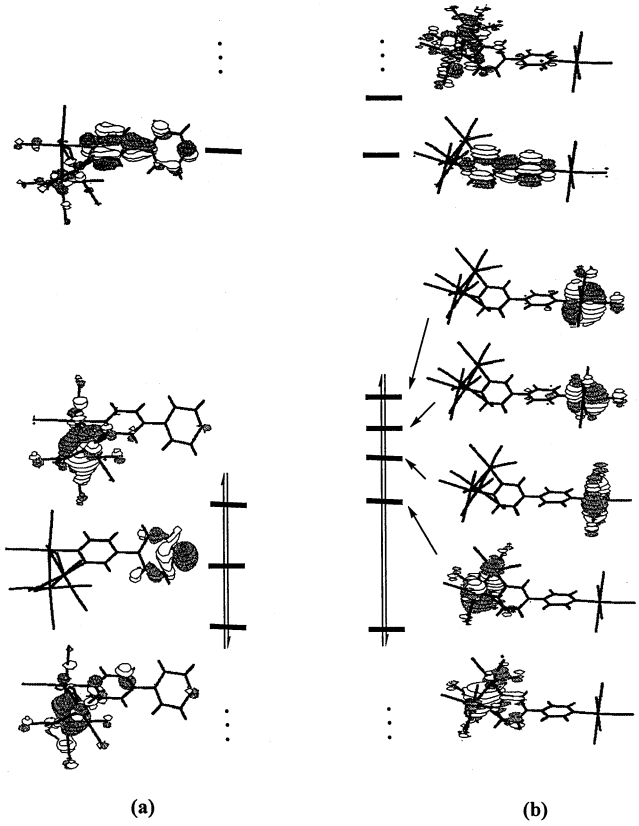

Fig. 4. The contour plots of the frontier molecular orbitals for (a) **1** and (b) **3**.

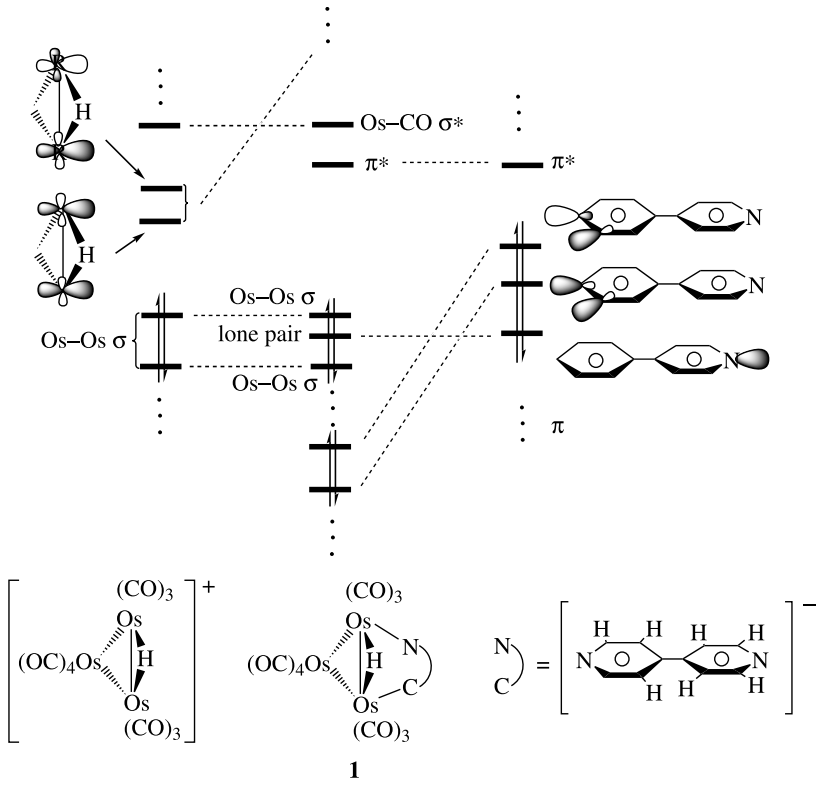

1

Fig. 5. The orbital interaction diagram between the $[HOs_3(CO)_{10}]^+$ fragment (left) and the dipyridyl ligand (right) in **1**.

with those corresponding to the lone pair orbitals on the two nitrogen atoms and the unsubstituted carbon. The central column illustrates clearly how the HOMO–LUMO orbitals are derived. Fig. 6 provides an orbital interaction diagram for **3**. The diagram depicts how the molecular orbitals of **3** are derived from the orbital interactions between **1** and the $W(CO)_5$ fragment. In addition to the three 't_{2g}' set orbitals, the $W(CO)_5$ fragment has an empty σ-accepting orbital for interaction with the lone pair orbital from the uncoordinated nitrogen in **1**. The orbital interaction between the two structural moieties features a simple two-orbital model in which the uncoordinated nitrogen of **1** provides a σ-donor while $W(CO)_5$ acts as a σ-acceptor.

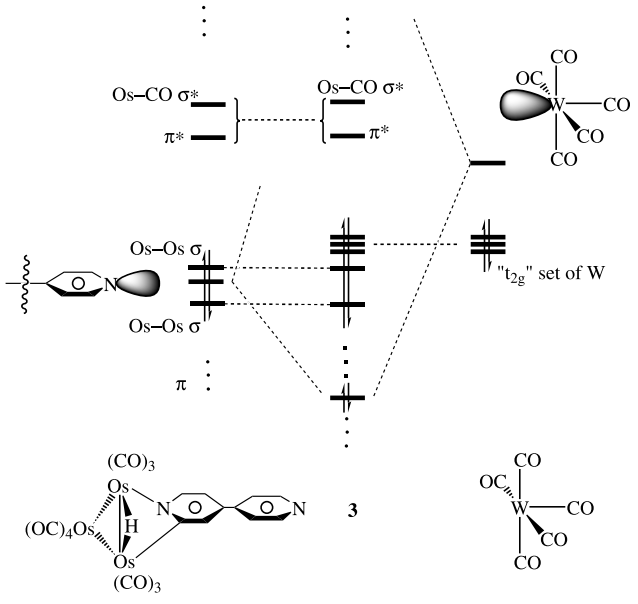

Fig. 6. The orbital interaction diagram between compound **1** (left) and the $W(CO)_5$ fragment (right) in **3**.

The orbital characteristics found in the HOMO–LUMO regions for **1**–**3** allow us to conclude that the lowest electronic transitions for these clusters are related to metal-to-ligand charge transfer transitions. The high intensity in the absorption peaks observed from UV–vis data is consistent with these calculation results. For **1** and **2**, the charge transfer arises probably from the Os–Os bonding d electrons to the π* empty orbitals of the dipyridyl ligand. For the heteronuclear complex **3**, the charge transfer is, however, expected to occur from the tungsten metal centre. The molecular orbital calculations show that the HOMO–LUMO gap is the smallest for **3**, due to the inclusion of the 't_{2g}' set orbital of the $W(CO)_5$ unit in the HOMO–LUMO region. The calculated HOMO–LUMO gaps for the three clusters are in the order of **3** (2.74 eV) < **2** (3.31 eV) < **1** (3.62 eV). Compound **2** has a smaller energy gap than that of **1**, suggesting that linking two Os_3 cluster units gives a greater degree of delocalization.

3. Conclusion

Starting with the metalloligand $[Os_3(\mu\text{-}H)(CO)_{10}(\mu\text{-}NC_5H_3C_5H_4N)]$ (**1**), some new heterometallic osmium carbonyl clusters containing a dipyridyl bridge were prepared and spectroscopically characterized. Structurally, these complexes contain a trinuclear cluster unit covalently appended to another transition metal carbonyl moiety by a 4,4′-dipyridyl bridge. Theoretical investigations based on density functional theory revealed that introduction of the $W(CO)_5$ fragment to **1** imposes a significant electronic effect on the energies of the frontier orbitals and cluster **3** essentially has the 't_{2g}' set orbitals of the $W(CO)_5$ unit as the HOMO orbitals, in contrast to that found in **1**. The origin of the HOMO and the LUMO is comparable for **1** and **2**. This work not only constitutes a new generation of transition metal carbonyl cluster research but also opens up an important branch in the construction of metallosupramolecular assemblies.

4. Experimental

4.1. General procedures

All reactions were carried out under N_2 with the use of standard inert atmosphere and Schlenk techniques, but no special precautions were taken to exclude oxygen during work-up. Solvents were predried and distilled from appropriate drying agents [19]. All chemicals, unless otherwise stated, were obtained from commercial sources and used as received. Preparative TLC was performed on 0.7 mm silica plates (Merck Kieselgel 60 GF_{254}) prepared in our laboratory. The starting materials $[Os_3(CO)_{10}(NCMe)_2]$ [20] and $[ReCl(CO)_3(4,4'\text{-bipy})_2]$ [9b] were prepared by reported procedures. Infrared spectra were recorded as CH_2Cl_2 solutions in a CaF_2 cell (0.5 mm path length) on a Perkin–Elmer Paragon 1000 PC or Nicolet Magna 550 Series II FTIR spectrometer. Proton NMR spectra were measured in $CDCl_3$ on a Varian INOVA 400 MHz FT NMR spectrometer. Chemical shifts were quoted relative to $SiMe_4$ ($\delta = 0$). Fast atom bombardment mass spectra were recorded on a Finnigan MAT SSQ710 mass spectrometer. Electronic absorption spectra were obtained with a Hewlett Packard 8453 UV–vis spectrometer. Cyclic voltammetry experiments were done with a Princeton Applied Research (PAR) model 273A potentiostat. A conventional three-electrode configuration consisting of a glassy-carbon working electrode, a Pt-wire counter electrode and a $Ag/AgNO_3$ reference electrode (0.1 M in MeCN) was used. The solvent in all measurements was deoxygenated CH_2Cl_2 and the supporting electrolyte was 0.1 M $[Bu_4N]PF_6$. Ferrocene was added as a calibrant after each set of measurements and all potentials reported were quoted with reference to the ferrocene–ferrocenium couple. For DFT calculations at the B3LYP level, the basis set used for C, N, O and H atoms was 6–31G [21] while an effective core potential with a LanL2DZ basis set [22] was employed for Os atoms.

4.2. Complex preparations

4.2.1. Synthesis of $[Os_3(\mu\text{-}H)(CO)_{10}(\mu\text{-}NC_5H_3C_5H_4N)]$ (1) and $[Os_3(\mu\text{-}H)(CO)_{10}(\mu\text{-}NC_5H_3C_5H_3N)Os_3(\mu\text{-}H)(CO)_{10}]$ (2)

4.2.1.1. Method 1: Stoichiometric reaction of $[Os_3(CO)_{10}(NCMe)_2]$ with 4,4′-bipy. Equal molar amounts of $[Os_3(CO)_{10}(NCMe)_2]$ (40.0 mg, 0.043 mmol) and 4,4′-bipy (6.7 mg, 0.043 mmol) were mixed and dissolved in CH_2Cl_2 (25 ml). The yellow solution was stirred at room temperature (r.t.). After stirring for 1 h, the resulting mixture was concentrated to about 3 ml. Subsequent TLC separation eluting with C_6H_{14}–CH_2Cl_2 (1:1, v/v) gave a major deep yellow band ($R_f = 0.70$) which was isolated and identified as the dimeric product **2** after recrystallization from CH_2Cl_2 (50%, 20.0 mg). The minor yellow band ($R_f = 0.10$) afforded compound **1** in 10% yield (4.3 mg). For **1**: Anal. Found: C, 23.50; H, 0.69; N, 2.52. $C_{20}H_8N_2O_{10}Os_3$ requires: C, 23.86; H, 0.80; N, 2.78%. For **2**: Anal. Found: C, 19.12; H, 0.34; N, 1.45. $C_{30}H_8N_2O_{20}Os_6$ requires: C, 19.40; H, 0.43; N, 1.51%.

4.2.1.2. Method 2: Reaction of $[Os_3(CO)_{10}(NCMe)_2]$ with excess 4,4′-bipy. The overall yield of **1** can be greatly enhanced by adopting the following procedures. A fivefold excess of 4,4′-bipy (33.5 mg, 0.21 mmol) was dissolved in CH_2Cl_2 (25 ml) and the solution was kept at 0 °C. To this solution was added dropwise a CH_2Cl_2 solution (10 ml) of $[Os_3(CO)_{10}(NCMe)_2]$ (40.0 mg, 0.043 mmol) via a dropping funnel at 0 °C over a period of 15 min. Work-up as described above gave **1** in 65% yield (28.1 mg) while that of **2** in 15% yield (6.0 mg).

4.2.2. Synthesis of $[Os_3(\mu\text{-}H)(CO)_{10}(\mu\text{-}NC_5H_3C_5H_4N)W(CO)_5]$ (3)

$W(CO)_6$ (14.1 mg, 0.04 mmol) was suspended in dry THF (15 ml) in a flask fitted with a condenser jacket. The mixture was then irradiated with a 125 W, medium-pressure mercury lamp whilst being stirred for about 0.5 h, until a golden yellow solution corresponding to $[W(CO)_5(THF)]$ was obtained. The solution mixture was filtered through a pad of celite with a sintered glass funnel and one molar equivalent of **1** (37.3 mg, 0.04 mmol) was subsequently added. The yellow solution was stirred for 2 h and then evaporated to dryness. The residue was subjected to preparative TLC over silica using C_6H_{14}–CH_2Cl_2 (1:1, v/v) as eluent to afford **3** as a

yellow solid ($R_f = 0.65$) in 45% yield (24.0 mg). Anal. Found: C, 22.38; H, 0.53; N, 2.12. $C_{25}H_8N_2O_{15}Os_3W$ requires: C, 22.56; H, 0.61; N, 2.11%.

4.2.3. Synthesis of $[ReCl(CO)_3\{Os_3(\mu\text{-}H)(CO)_{10}(\mu\text{-}NC_5H_3C_5H_4N)\}_2]$ (4)

4.2.3.1. Method 1: Reaction of $[Os_3(CO)_{10}(NCMe)_2]$ with $[ReCl(CO)_3(4,4'\text{-bipy})_2]$. Two equivalents of **1** (40.0 mg, 0.043 mmol) was reacted with $[ReCl(CO)_3(4,4'\text{-bipy})_2]$ (13.3 mg, 0.021 mmol) in CH_2Cl_2 (25 ml) for 2 h at r.t. The resulting yellow solution was purified by TLC eluting with C_6H_{14}–CH_2Cl_2 (4:6, v/v) to afford a yellow band ($R_f = 0.30$) identified as **4** in 58% yield (28.8 mg). Anal. Found: C, 22.04; H, 0.59; N, 2.12. $C_{43}H_{16}N_4O_{23}ClOs_6Re$: requires C, 22.27; H, 0.70; N, 2.42%.

*4.2.3.2. Method 2: Reaction of **1** with $[ReCl(CO)_5]$.* A mixture of **1** (30.2 mg, 0.030 mmol) and $[ReCl(CO)_5]$ (5.4 mg, 0.015 mmol) was dissolved in C_6H_6 (25 ml) and the solution was brought to reflux for 3 h. Purification of the resulting yellow suspension was achieved by TLC using C_6H_{14}–CH_2Cl_2 (4:6, v/v) as eluent to give **4** in 54% yield (18.7 mg).

5. Crystallography

Single crystals of **1** and **2** suitable for X-ray crystallographic analyses were grown by evaporation of their respective solutions in C_6H_{14}–CH_2Cl_2 and those of **3**·$CHCl_3$ in cyclohexane–$CHCl_3$ at r.t. Crystal data and other experimental details are summarized in Table 4. The diffraction experiments were carried out at room temperature either on a Rigaku AFC7R (**1**) or a Bruker Axs SMART 1000 CCD area-detector (**2** and **3**) diffractometer using graphite-monochromated Mo–K_α radiation ($\lambda = 0.71073$ Å). Unit-cell parameters for **1** were determined from 25 accurately centred reflections. The intensity data were corrected for Lorentz and polarization effects. Absorption corrections by the ψ-scan method were applied [23]. Cell parameters and orientation matrix for **2** and **3** were obtained from the least-squares refinement of reflections measured in three different sets of 15 frames each. The collected frames were processed with the software SAINT [24a] and an absorption correction was applied (SADABS [24b]) to the collected reflections.

The space groups for all crystals were determined from a combination of Laue symmetry check and their systematic absences, which were then confirmed by successful refinement of the structures. The structures were solved by direct methods (SIR-92 [25] for **1** and **3**, SHELXTL [26] for **2**) in conjunction with standard

Table 4
Summary of crystal structure data for complexes **1**–**3**

	1	**2**	**3**·$CHCl_3$
Empirical formula	$C_{20}H_8N_2O_{10}Os_3$	$C_{30}H_8N_2O_{20}Os_6$	$C_{26}H_9N_2Cl_3O_{15}Os_3W$
Molecular weight	1006.89	1857.58	1450.17
Crystal size (mm)	0.34 × 0.32 × 0.17	0.35 × 0.32 × 0.29	0.36 × 0.35 × 0.26
Crystal system	Monoclinic	Monoclinic	Monoclinic
Space group	$P2_1/c$	$C2/c$	$P2_1/c$
a (Å)	9.320(4)	35.636(7)	9.576(1)
b (Å)	12.904(4)	7.788(2)	20.845(1)
c (Å)	21.175(5)	16.984(3)	20.978(1)
α (°)			
β (°)	92.86(3)	104.55(3)	95.50(2)
γ (°)			
U (Å^3)	2543(1)	4562(2)	4167.9(5)
Z	4	4	4
μ (Mo–K_α)/cm^{-1}	149.94	167.15	121.15
F(000)	1800	3272	2608
$2\theta_{max}$ (°)	50.0	55.1	55.1
Reflections collected	4998	13016	24777
Unique reflections	4691	5116	9669
R_{int}	0.073	0.0546	0.044
Observed reflections [$I > n\sigma(I)$]	3027 ($n = 1.5$)	5116 ($n = 2.0$)	6250 ($n = 1.5$)
No. of parameters	156	266	447
Residuals	$R_1 = 0.057$	$R_1 = 0.0382$	$R_1 = 0.063$
	$R_w = 0.062$	$wR_2 = 0.1002$	$R_w = 0.069$
Goodness-of-fit	2.90	1.002	1.96
Residual extrema in final diff. map (e Å^{-3})	3.39 to −1.43	1.974 to −1.732	1.62 to −0.58

Fourier difference techniques and subsequently refined by full-matrix least-squares analyses. Except for the $CHCl_3$ molecules in the structure of **3**, all the non-hydrogen atoms were refined with anisotropic displacement parameters. The positions of the hydride ligands were located from Fourier difference maps and all other hydrogen atoms were placed in their ideal positions but not refined. For **3**, the two $CHCl_3$ solvates were modeled with occupancy factors of 0.5 each. The highest residual electron density peaks are all in the vicinity of the heavy atoms (Os and W).

6. Supplementary material

Crystallographic data (comprising hydrogen atom coordinates, thermal parameters and full tables of bond lengths and angles) for the structural analysis has been deposited with the Cambridge Crystallographic Centre (Deposition No. 177829 to 177831). Copies of this information may be obtained free of charge from The Director, CCDC, 12 Union Road, Cambridge, CB2 1EZ, UK (Fax: +44-1223-336-033; e-mail: deposit@ccdc.cam.ac.uk or www: http://www.ccdc.cam.ac.uk).

Acknowledgements

Financial support from the Hong Kong Baptist University is gratefully acknowledged.

References

[1] (a) A.E. Martell, R.D. Hancock, Metal Complexes in Aqueous Solution, Plenum, New York, 1996;
(b) J.M. Lehn, Supramolecular Chemistry, VCH, Weinheim, 1995;
(c) E.C. Constable, Prog. Inorg. Chem. 42 (1994) 67;
(d) C. Janiak, L. Uehlin, H.-P. Wu, P. Klüfers, H. Piotrowski, T.G. Scharmann, J. Chem. Soc. Dalton Trans. (1999) 3121;
(e) H.-P. Wu, C. Janiak, G. Rheinwald, H. Lang, J. Chem. Soc. Dalton Trans. (1999) 183;
(f) S. Leininger, B. Olenyuk, P.J. Stang, Chem. Rev. 100 (2000) 853;
(g) S.J. Loeb, S.L. Murphy, J.A. Wisner, Cryst. Eng. 2 (1999) 27.

[2] (a) M.D. Ward, Chem. Soc. Rev. (1995) 121 (and references cited therein);
(b) L.-M. Zheng, X. Fang, K.-H. Lii, H.-H. Song, X.-Q. Xin, H.-K. Fun, K. Chinnakali, I.A. Razak, J. Chem. Soc. Dalton Trans. (1999) 2311;
(c) J. Hock, A.M.W. Cargill Thompson, J.A. McCleverty, M.D. Ward, J. Chem. Soc. Dalton Trans. (1996) 4257;
(d) V.W.-W. Yam, V.C.-Y. Lau, K.-K. Cheung, J. Chem. Soc. Chem. Commun. (1995) 259.

[3] (a) C. Creutz, Prog. Inorg. Chem. 30 (1983) 1;
(b) O.M. Yaghi, G. Li, Angew. Chem. Int. Ed. Engl. 34 (1995) 207;
(c) A.J. Blake, S.J. Hill, P. Hubberstey, W.-S. Li, J. Chem. Soc. Dalton Trans. (1998) 909;
(d) R.V. Slone, J.T. Hupp, C.L. Stern, T.E. Albrecht-Schmitt, Inorg. Chem. 35 (1996) 4096;
(e) J. Lu, C. Yu, T. Niu, T. Paliwala, G. Crisci, F. Somosa, A.J. Jacobson, Inorg. Chem. 37 (1998) 4637;
(f) M. Kondo, T. Yoshitomi, K. Seki, H. Matsuzaka, S. Kitagawa, Angew. Chem. Int. Ed. Engl. 36 (1997) 1725.

[4] (a) R. Horikoshi, T. Mochida, N. Maki, S. Yamada, H. Moriyama, J. Chem. Soc. Dalton Trans. (2002) 28;
(b) L. Carlucci, G. Ciani, P. Macchi, D.M. Proserpio, Chem. Commun. (1998) 1837;
(c) A.J. Blake, N.R. Champness, A. Khlobystov, D.A. Lemenovskii, W.-S. Li, M. Schröder, Chem. Commun. (1997) 2027;
(d) O.M. Yaghi, H. Li, T.L. Groy, Inorg. Chem. 36 (1997) 4292;
(e) O.M. Yaghi, H. Li, J. Am. Chem. Soc. 118 (1996) 295;
(f) S. Subramanian, M.J. Zaworotko, Angew. Chem. Int. Ed. Engl. 34 (1995) 2127;
(g) M.L. Tong, B.H. Ye, J.W. Cai, X.-M. Chen, S.W. Ng, Inorg. Chem. 37 (1998) 2645.

[5] W.-Y. Wong, S.-H. Cheung, S.-M. Lee, S.-Y. Leung, J. Organomet. Chem. 596 (2000) 36.

[6] (a) W.-Y. Wong, W.-T. Wong, S.-Z. Hu, Inorg. Chim. Acta 234 (1995) 5;
(b) W.-Y. Wong, W.-T. Wong, K.-K. Cheung, J. Chem. Soc. Dalton Trans. (1995) 1379;
(c) W.-Y. Wong, W.-T. Wong, J. Chem. Soc. Dalton Trans. (1996) 3209.

[7] (a) C.C. Yin, A.J. Deeming, J. Chem. Soc. Dalton Trans. (1975) 2091;
(b) A.J. Deeming, R. Peters, M.B. Hursthouse, J.D.J. Backer-Dirks, J. Chem. Soc. Dalton Trans. (1982) 787.

[8] (a) J.T. Lin, S.-S. Sun, J.J. Wu, L. Lee, K.-J. Lin, Y.F. Huang, Inorg. Chem. 34 (1995) 2323;
(b) S. Sakanishi, D.A. Bardwell, S. Couchman, J.C. Jeffery, J.A. McCleverty, M.D. Ward, J. Organomet. Chem. 528 (1997) 35;
(c) M.M. Zulu, A.J. Lees, Inorg. Chem. 27 (1988) 1139.

[9] (a) D.R. Gamelin, M.W. George, P. Glyn, F.-W. Grevels, F.P.A. Johnson, W. Klotzbücher, S.L. Morrison, G. Russell, K. Schaffner, J.J. Turner, Inorg. Chem. 33 (1994) 3246;
(b) P.J. Giordano, M.S. Wrighton, J. Am. Chem. Soc. 101 (1979) 2888;
(c) V.W.-W. Yam, V.C.-Y. Lau, K.-Z. Wang, K.-K. Cheung, C.-H. Huang, J. Mater. Chem. 8 (1998) 89;
(d) O. Briel, K. Sünkel, I. Krossing, H. Nöth, E. Schmälzlin, K. Meerholz, C. Bräuchle, W. Beck, Eur. J. Inorg. Chem. (1999) 483;
(e) M.W. George, F.P.A. Johnson, J.R. Westwell, P.M. Hodges, J.J. Turner, J. Chem. Soc. Dalton Trans. (1993) 2977.

[10] W.-Y. Wong, W.-T. Wong, J. Chem. Soc. Dalton Trans. (1996) 1853.

[11] A.J. Arce, C. Acuña, A.J. Deeming, J. Organomet. Chem. 356 (1988) C47.

[12] C.S. Kraihanzel, F.A. Cotton, Inorg. Chem. 2 (1963) 533.

[13] S.T. Beatty, B. Bergman, E. Rosenberg, W. Dastru, R. Gobetto, L. Milone, A. Viale, J. Organomet. Chem. 593–594 (2000) 226.

[14] G.L. Geoffroy, M.S. Wrighton (Eds.),Organometallic Photochemistry, Academic Press, New York, 1979.

[15] E. Rosenberg, M.J. Abedin, D. Rokhsana, D. Osella, L. Milone, C. Nervi, J. Fiedler, Inorg. Chim. Acta 300–302 (2000) 769.

[16] S.E. Kabir, C.A. Johns, K.M. Abdul Malik, A. Abdul Mottalib, E. Rosenberg, J. Organomet. Chem. 625 (2001) 112.

[17] M.J. Calhorda, E. Hunstock, L.F. Veiros, Eur. J. Inorg. Chem. (2001) 223.

[18] G. Schaftenaar, Molden ver. 3.5, CAOS/CAMM Center Nijmegen, Toernooiveld, Nijmegen, The Netherlands, 1999.

[19] W.L.F. Armarego, D.D. Perrin, Purification of Laboratory Chemicals, 4th ed., Butterworth-Heinemann, Guildford, 1996.

[20] J.N. Nicholls, M.D. Vargas, Inorg. Synth. 28 (1990) 289.

[21] P.C. Hariharan, J.A. Pople, Theor. Chim. Acta 28 (1973) 213.
[22] P.J. Hay, W.R. Wadt, J. Chem. Phys. 82 (1985) 299.
[23] A.C.T. North, D.C. Phillips, F.S. Mathews, Acta Crystallogr. Sect. A. 24 (1968) 351.
[24] (a) SAINT, Reference manual, Siemens Energy and Automation, Madison, WI, 1994–1996;
(b) G.M. Sheldrick, SADABS, Empirical Absorption Correction Program, University of Göttingen, 1997.
[25] G.M. Sheldrick, in: G.M. Sheldrick, C. Kruger, R. Goddard (Eds.), Crystallographic Computing 3, Oxford University Press, London, 1985, p. 175.
[26] G.M. Sheldrick, SHELXTL™, Reference manual, ver. 5.1, Madison, WI, 1997.